Available online at www.sciencedirect.com

Cement and Concrete Research 37 (2007) 54 – 62

# Experimental and numerical study of electrochemical chloride removal from brick and concrete specimens

A. Toumi [a,*], R. François [b], O. Alvarado [b,c]

[a] Institut Universitaire de Technologie, Toulouse, France
[b] Institut National des Sciences Appliquées, Toulouse, France
[c] Université Paul Sabatier, Toulouse, France

Received 24 May 2005; accepted 19 September 2006

## Abstract

The electrochemical technique for chloride extraction (desalination) was applied in galvanostatic mode to cylindrical brick and concrete specimens with a steel bar as reinforcement placed in the centre. The specimens were initially contaminated by immersion in a solution of 35 g/l NaCl. Based on the Nernst–Planck equations, a numerical model was developed considering the interactions between the various ionic species in the pore solution. The model makes it possible to predict the evolution of the chloride profile with time. The numerical and experimental results are compared and the model parameters discussed.

*Keywords:* Brick; Concrete(E); Diffusion(C); Chloride(D); Migration; Modelling

## 1. Introduction

Corrosion of steel reinforcement in contact with chloride ions is one of the major causes of degradation of reinforced concrete structures throughout the world. The deterioration induced is characterized by a reduction of the cross-section of the embedded steel and loss of the bond between steel and concrete. For new structures, protective methods such as galvanizing of the reinforcements [1–3], epoxy coating of steels [4] or addition of inhibitors [5] are used where there is a risk of rebar corrosion. In the case of old structures, repair techniques remain essential for rehabilitating corroded parts. Among the methods available is chloride extraction, also called desalination, by application of an electric field [6–10]. This method involves the application of a high current density for a short period, typically a few weeks. The steel reinforcement acts as the cathode, and an extended anode is placed in a suitable electrolyte at the concrete surface. The steel cathode repels anions and attracts cations in the concrete pore solution. Therefore, sodium and potassium accumulate at the cathode. This accumulation has been shown to increase the risk of an alkali–silica reaction in concrete containing potentially reactive aggregates [9].

The present work aims at analyzing the transport of ionic species in a saturated medium in order to predict the accumulation of alkaline species near the embedded steel and to define a time criterion for the efficiency of the technique. A model based on a multi-species approach is presented. Moreover, in order to validate the numerical predictions, a desalination programme was conducted on both cylindrical brick and concrete specimens for various periods. The inert material (brick) was chosen for two reasons: (i) to avoid binding between chloride and the matrix, which is dominant in the case of concrete specimens, and (ii) to limit the number of chemical species to be taken into account in the computation. Thus, the model was tested in a simple case before performing simulations with concrete.

## 2. Theoretical background

### 2.1. Basic equations

According to irreversible thermodynamics and assuming that the activity coefficient is equal to the concentration, the

---

[*] Corresponding author. Laboratoire Matériaux et Durabilité des Constructions, INSA–UPS, 135 Av. de Rangueil, 31077 Toulouse cedex4, France. Tel.: +33 561 55 99 19; fax: +33 561 55 99 49.

*E-mail address:* toumi@insa-toulouse.fr (A. Toumi).

0008-8846/$ - see front matter © 2006 Elsevier Ltd. All rights reserved.
doi:10.1016/j.cemconres.2006.09.012

diffusion process in saturated porous media can be completely described through the following set of extended Nernst–Planck equations [11–20]:

$$J_i = -\left[D_i \nabla C_i + z_i D_i C_i \frac{F}{RT} \nabla \phi\right] \tag{1}$$

$$\nabla \phi = -\frac{RT}{F} \frac{(I_c/F) + \sum_i z_i D_i \nabla C_i}{\sum_i z_i^2 D_i C_i} \tag{2}$$

where $J_i$ is the flux of the ion $i$ (mol m$^{-2}$ s$^{-1}$), $D_i$ the diffusion coefficient (m$^2$ s$^{-1}$), $C_i$ the concentration (mol m$^{-3}$), $z_i$ the valence of the ion, $F$ Faraday's constant (C mol$^{-1}$), $R$ the gas constant (J K mol$^{-1}$), $T$ the temperature (K), $\phi$ the electric potential (V) and $I_c$ the current density (A m$^{-2}$).

In the case of porous material, the continuity equation and the electroneutrality can be expressed as follows:

$$p\frac{\partial C_i}{\partial t} + (1-p)\rho\frac{\partial B_i}{\partial t} = -\nabla \cdot J_i \tag{3}$$

$$\sum_i z_i C_i = 0 \tag{4}$$

where $p$ is the porosity, $\rho$ is the density of the material (kg m$^{-3}$) and $B_i$ is the quantity of the bound species (mol kg$^{-1}$).

### 2.2. Mathematical treatment

The above non-linear differential equations are solved by assuming a radial ingress process in a cylindrical geometry with radius $R$. In order to solve the coupled equations numerically, the following dimensionless variables are introduced:

$$\hat{r} = \frac{r}{R}; \hat{t} = \frac{D_0.t}{R^2}; \hat{D}_i = \frac{D_i}{D_0}; \hat{C}_i = \frac{C_i}{C_0}; \hat{I}_c = \frac{I_c.R}{F.D_0.C_0}; \hat{J}_i \frac{J_i.R}{D_0 C_0}; \hat{\phi} = \frac{F.\phi}{R.T}$$

Taking into account the above set of variables, the new transformed system of equations to be solved is:

$$\hat{J}_i = -\left[\hat{D}_i \frac{\partial \hat{C}_i}{\partial \hat{r}} + z_i \hat{D}_i \hat{C}_i \frac{\partial \hat{\phi}}{\partial \hat{r}}\right] \tag{5}$$

$$\frac{\partial \hat{\phi}}{\partial \hat{r}} = -\frac{\hat{I}_c + \sum_i z_i \hat{D}_i \frac{\partial \hat{C}_i}{\partial \hat{r}}}{\sum_i z_i^2 \hat{D}_i \hat{C}_i} \tag{6}$$

$$p\frac{\partial \hat{C}_i}{\partial \hat{t}} + (1-p)\rho\frac{\partial \hat{B}_i}{\partial \hat{t}} = -\frac{1}{\hat{r}}\frac{\partial}{\partial \hat{r}}(\hat{r}\,.\hat{J}_i) \tag{7}$$

The simulations made in the framework of this work were performed by considering the major ionic species in the pore solution. Therefore, according to the measured pore solution composition of the concrete studied (cf. Section 4), the following species were considered: sodium ($Na^+$), potassium ($K^+$), calcium ($Ca^{2+}$) chloride ($Cl^-$) and hydroxide ($OH^-$).

During the transport processes, the bound chloride ions in the solid phase were accounted for in the calculations by means of the Freundlich isotherm:

$$B_{Cl} = a(C_{Cl})^b \tag{8}$$

where $a$ and $b$ are empirical coefficients to be determined.

## 3. Experimental programme

The experimental study comprised two parts. The first one dealt with brick specimens (inert material) which provided a test of the model in simplified conditions. The simplified conditions consisted of:

(i) the number of species computed was limited ($Na^+$ and $Cl^-$), and
(ii) chloride binding was negligible.

In the second part, the concrete specimens were tested, corresponding to the real conditions in which the technique is used.

### 3.1. Specimens

Cylindrical brick specimens (100 mm in diameter and 50 mm in height) were cored from 50 × 400 × 400 mm blocs and then exposed to 35 g/l of NaCl for 48 h to obtain an initial chloride concentration uniformly distributed in the specimen. A steel bar 10 mm in diameter was inserted in the specimen to act as the cathode during the extraction process.

In order to investigate the concrete material, specimens (110 mm in diameter and 50 mm in height) were cast with a 10 mm centrally embedded steel bar. An ordinary Portland cement with a water/cement ratio of 0.47 was used. The mixture characteristics are given in Table 1.

The average 28-day compressive strength of the concrete studied was approximately 52 MPa. All the specimens were cured in a wet room (20 °C) for 28 days before their contamination. In order to accelerate the chloride penetration, a treatment over 390 days by means of cycles of three days of exposure to 35 NaCl g/l and 4 days of drying at 40 °C was used.

### 3.2. Chloride extraction procedure

The experimental setup for the Electrochemical Chloride Extraction (ECE) is described in Fig. 1. A titanium mesh anode

Table 1
Concrete mixture characteristics

| Materials | Mixture proportions (kg/m$^3$) |
|---|---|
| Cement (CPA CEM1 52.5R) | 310 |
| Water | 139.5 |
| Coarse aggregates | 1050 |
| Sand | 850 |
| Super plasticizer | 0.417 |

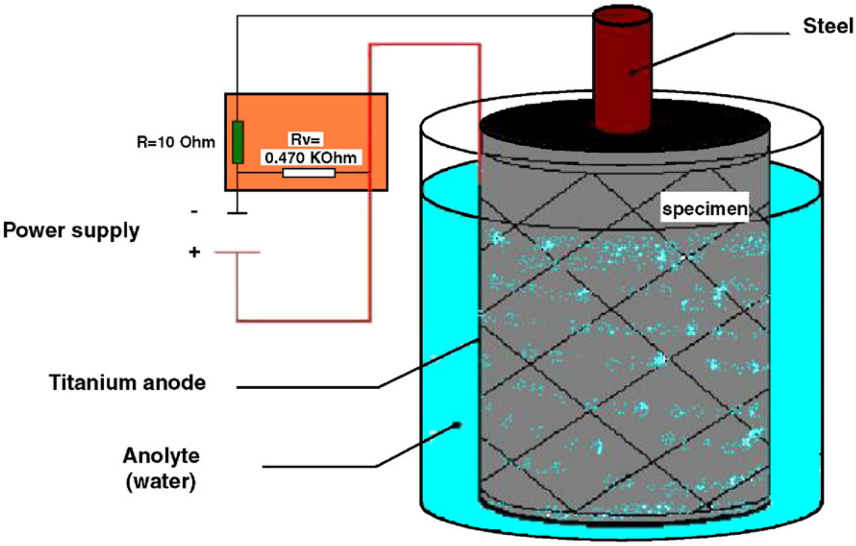

Fig. 1. Electrochemical chloride extraction setup.

was fixed on the surface of the specimen to provide electrical contact. An electrical resistance (10 Ω) was connected in series with the specimen in order to control the current density during the application of the technique. Distilled water was used as the anolyte.

A current density of 1 A/m$^2$ was applied to the brick specimens for 1, 3, 10 and 20 days. For the concrete specimens, two current densities (1 and 5 A/m$^2$) were investigated. Each current density was applied for 10, 20 or 31 days.

### 3.3. Chloride concentration profiles

At the end of the treatment, the specimens were removed from the ECE cell to measure the chloride concentration profiles. For that purpose, a conic sample was extracted from the tested specimen by sawing as sketched in Fig. 2. Then the sample was sectioned in slices and powdered for analysis. The total chloride concentration at a given depth was determined through potentiometric titration with 0.01 M $AgNO_3$ solution.

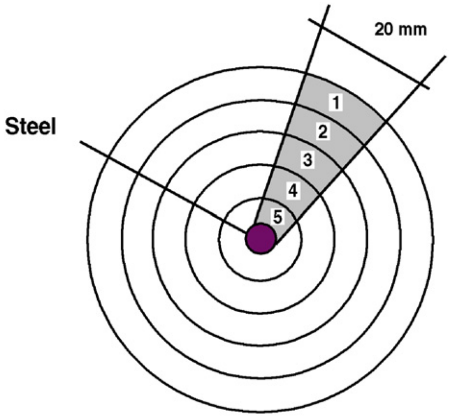

Fig. 2. Chloride profile determination procedure.

## 4. Input data for the model

### 4.1. Porosity and density

The porosity accessible to water and the density were measured on specimens of the same dimensions as those described in Section 3.1. Vacuum saturated water specimens were first weighed in water and in air. Then the samples were put in an oven at 105 °C to determine the dry weight. The values $p=0.196$ and $\rho=2440$ kg/m$^3$ were obtained for the brick specimens and $p=0.11$ and $\rho=2627$ kg/m$^3$ for the concrete specimens.

### 4.2. Concrete pore solution composition

The knowledge of the initial concentrations of the various ionic species in the material pore solution was necessary for the numerical simulations. In the case of brick material, the initial pore solution concentration corresponded to the total chloride determined by potentiometric titration in the absence of binding phenomena. However, in the case of concrete material, the determination of the concrete pore solution was not an easy task. In this work, the Pore Pressing Technique (PPT) [21] was used to provide the concentration of various species in the pore solution before and after their contamination. The results obtained are presented in Table 2.

Table 2
Concrete pore solution composition before and after contamination

| | pH | Composition (mol/l) | | | | | |
|---|---|---|---|---|---|---|---|
| | | $OH^-$ | $Cl^-$ | $Na^+$ | $K^+$ | $Ca^{2+}$ | $SO_4^{2-}$ |
| Before | 13.26 | 0.181 | 0.0018 | 0.0584 | 0.0454 | 0.04 | 0.0013 |
| After | 13.18 | 0.151 | 1.026 | 0.941 | 0.0496 | 0.099 | 0.003 |

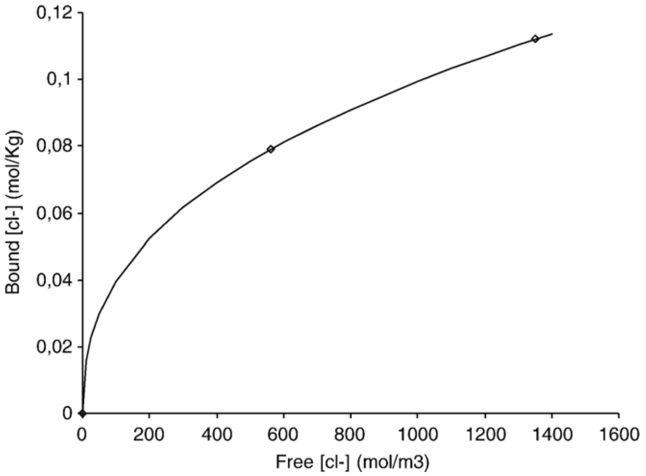

Fig. 3. Chloride binding isotherm.

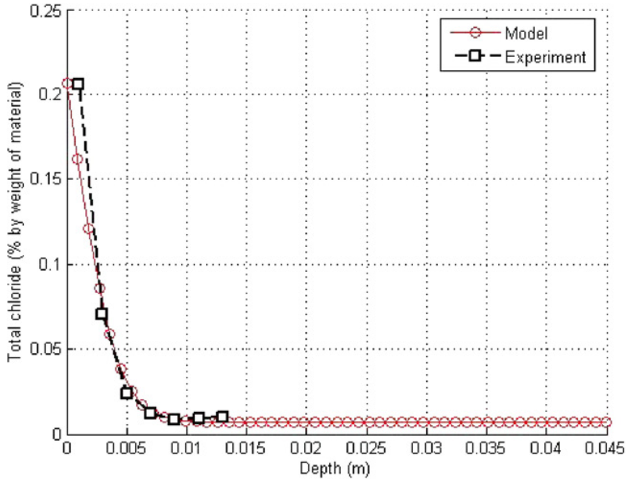

Fig. 4. Brick chloride content profile in immersion test (10 h of exposure).

### 4.3. Chloride binding isotherm

The chloride binding isotherm used in the numerical simulation was obtained according to the procedure proposed by Francy et al. [22]. Immersion tests in 35 and 80 g/l of NaCl solution were conducted on two samples simultaneously over a period of 137 days in order to reach an equilibrium state on the exposed surfaces of the specimens. At the end of the immersion, the total chloride concentrations on the exposed surfaces were determined by potentiometric titration, which enabled the chloride binding concentration to be calculated by assuming the porosity and the density of the concrete. The isotherm obtained is presented in Fig. 3. The measurements were fitted according to the Freundlich model to give $a=6.32.10^{-3}$ and $b=0.3988$ in Eq. (8).

### 4.4. Diffusion coefficients

If realistic simulations are to be performed, the diffusion coefficient of all the species must be known. However, the diffusion coefficients described in the model act as intrinsic ones, which makes their experimental determination difficult or even impossible. To make up for this lack of experimental data, the intrinsic diffusion coefficients of all the species taken into account in the model were estimated from the literature [11]. Table 3 gives the values of the diffusion coefficients used to perform the ECE simulations.

It must be emphasized that this set of coefficients must be also able to predict an immersion test. Figs. 4 and 5 show the comparison between numerical predictions and experimental data in the case of an immersion test conducted on specimens of the same geometry as those used in the ECE study. The brick and concrete specimens were exposed to 35 g/l of NaCl solution for 10 h and 137 days respectively. In the case of the concrete material, the simulations were performed using the concrete pore solution composition presented in Table 2 (before contamination).

Table 3
Values of the diffusion coefficient for the considered species

| Material | Diffusion coefficients (× $10^{-12}$ $m^2/s$) | | | | |
|---|---|---|---|---|---|
| | $OH^-$ | $Cl^-$ | $Na^+$ | $K^+$ | $Ca^{2+}$ |
| Brick | – | 80.6 | 16.6 | – | – |
| Concrete | 5 | 3 | 0.3 | 1 | 0.15 |

## 5. ECE results

### 5.1. Brick specimens

Fig. 6 shows the measured and computed concentration profiles of chloride ions within the material at four different times. For the current density applied (1 $A/m^2$), the ionic transport was dominated by diffusion. This was due to a strong porosity of the brick (19.6%) and the absence of binding. Concerning the efficiency of the ECE technique, it was found that the chloride content near the steel had been halved after 20 days of treatment.

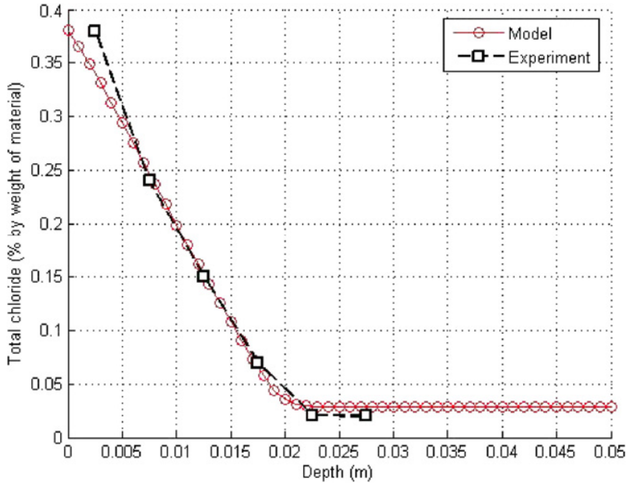

Fig. 5. Concrete chloride content profile in immersion test (137 days of exposure).

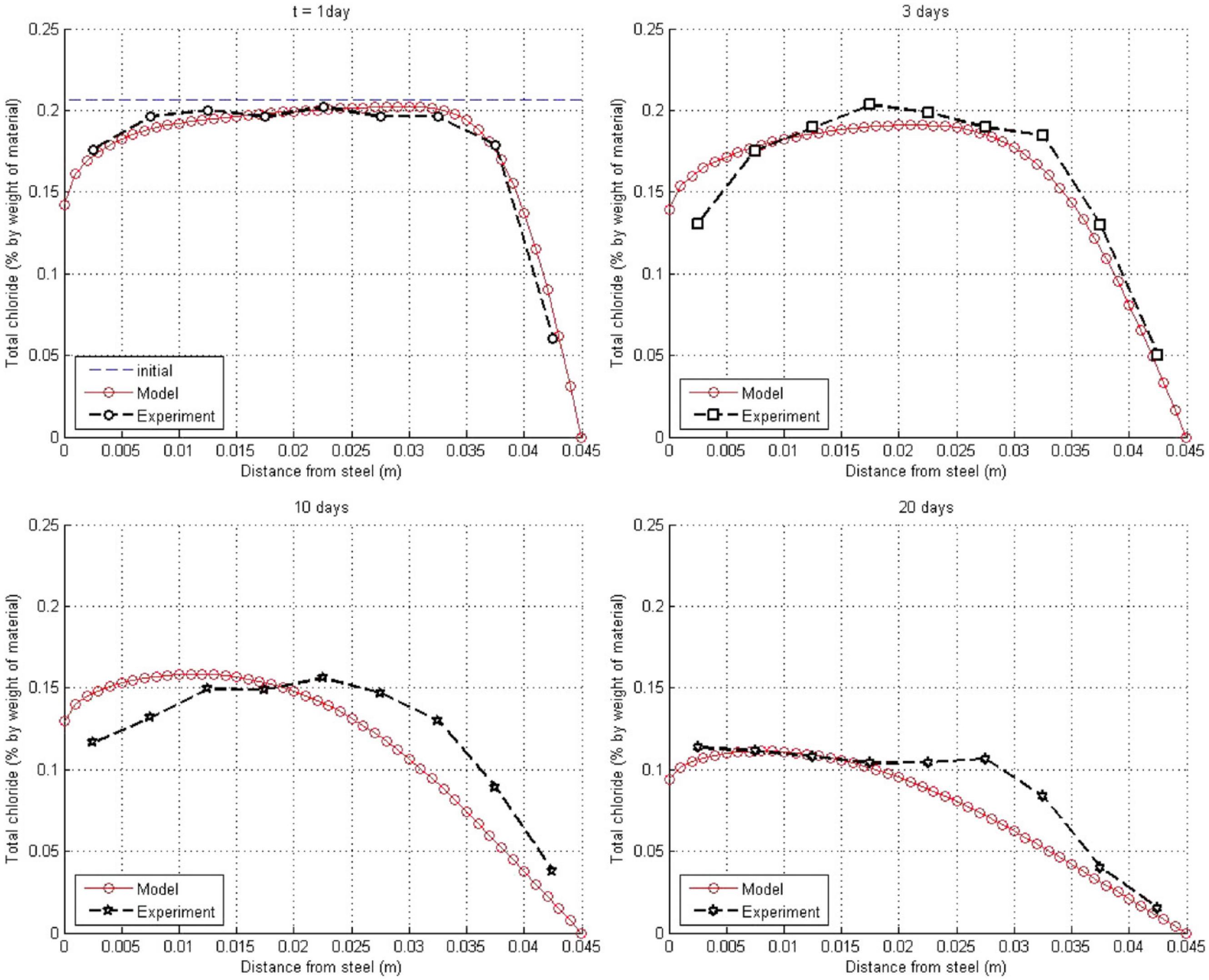

Fig. 6. Total chloride content profiles in brick specimens: diffusion process is the main impetus.

### 5.2. Concrete specimens

Fig. 7 shows the measured and computed total chloride content profiles with respect to the applied current densities of 1 and 5 A/m$^2$. There is a good correlation between the two sets of data. The model reproduces correctly the ionic movement in the concrete pore solution.

In contrast to the situation for brick, migration was the dominant transport mechanism. In the region close to the steel, it can be seen that the removal of chlorides was rapid at the beginning of the treatment and gradually became slower. This was due partly to a decrease in the potential gradient as a consequence of the increase in the amount of hydroxyl ions and cations near the steel. Fig. 8 illustrates the movement of the various species in the concrete pore solution during the treatment. One can note that, for the applied current density of 5 A/m$^2$, the free chloride content near the steel had decreased significantly after 10 and 31 days of treatment. In terms of total chloride, the reduction was limited because of the high capacity of the studied concrete to bind chloride ions.

Concerning the intensity of the current density, it can be seen that 5 A/m$^2$ applied for 10 days was more efficient in reducing the chloride content near the steel than 1 A/m$^2$ applied for 31 days. However, the concentration of cations in the region near the steel, in particular sodium and potassium ions, was greater for a high current density. This means that a risk of an alkali aggregate reaction process remains possible [9].

## 6. Conclusions

Electrochemical chloride removal investigation was conducted on both brick and concrete materials by associating experimental and numerical approaches. The following conclusions can be drawn from the present study:

1. The chloride removal and associated ionic movement in the pore solution can be reasonably predicted using the Nernst–Planck equation;
2. The ECE technique can significantly reduce the amount of chloride near the steel. However, the use of high current

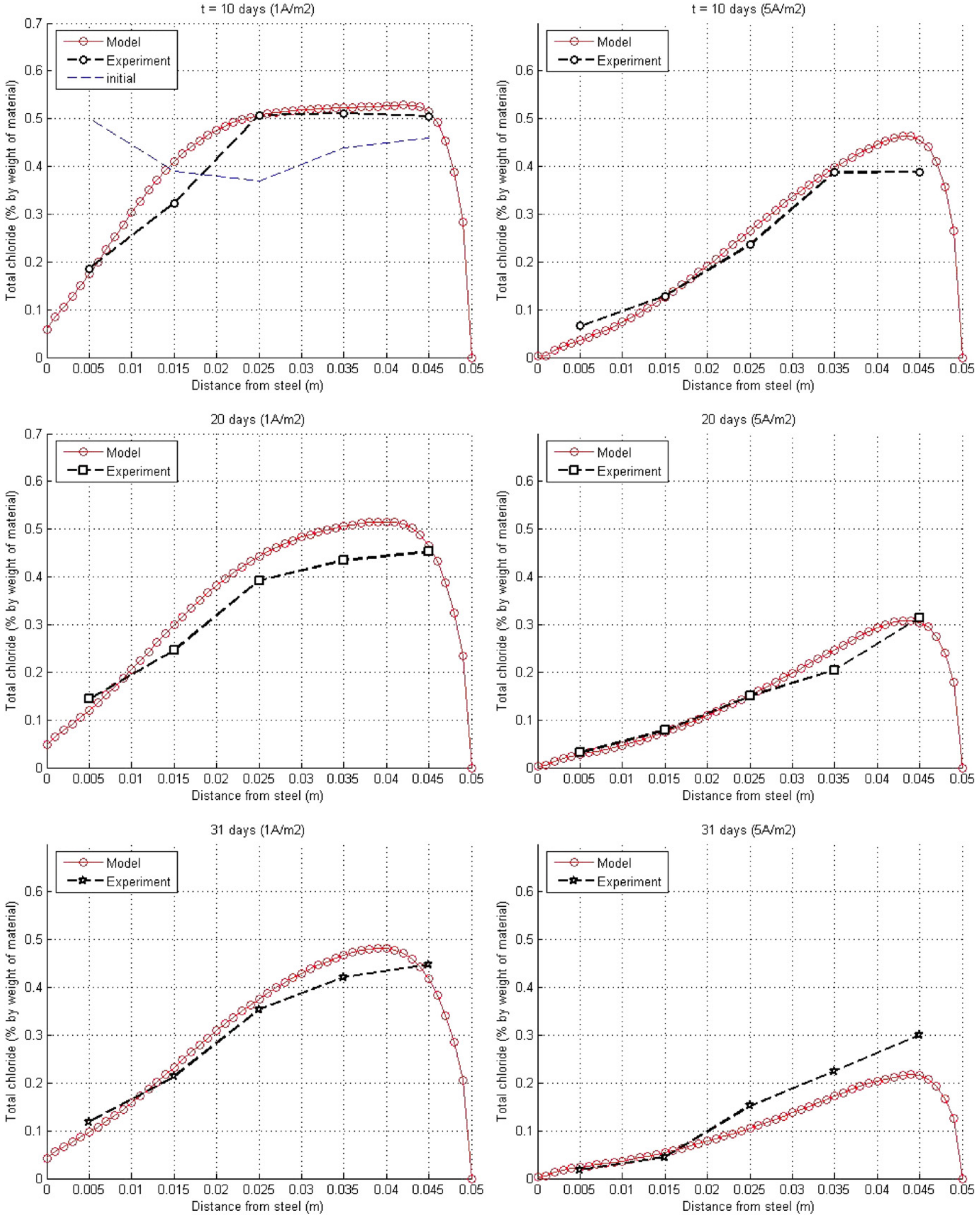

Fig. 7. Total chloride content profiles in mortar specimens: migration is the main impetus.

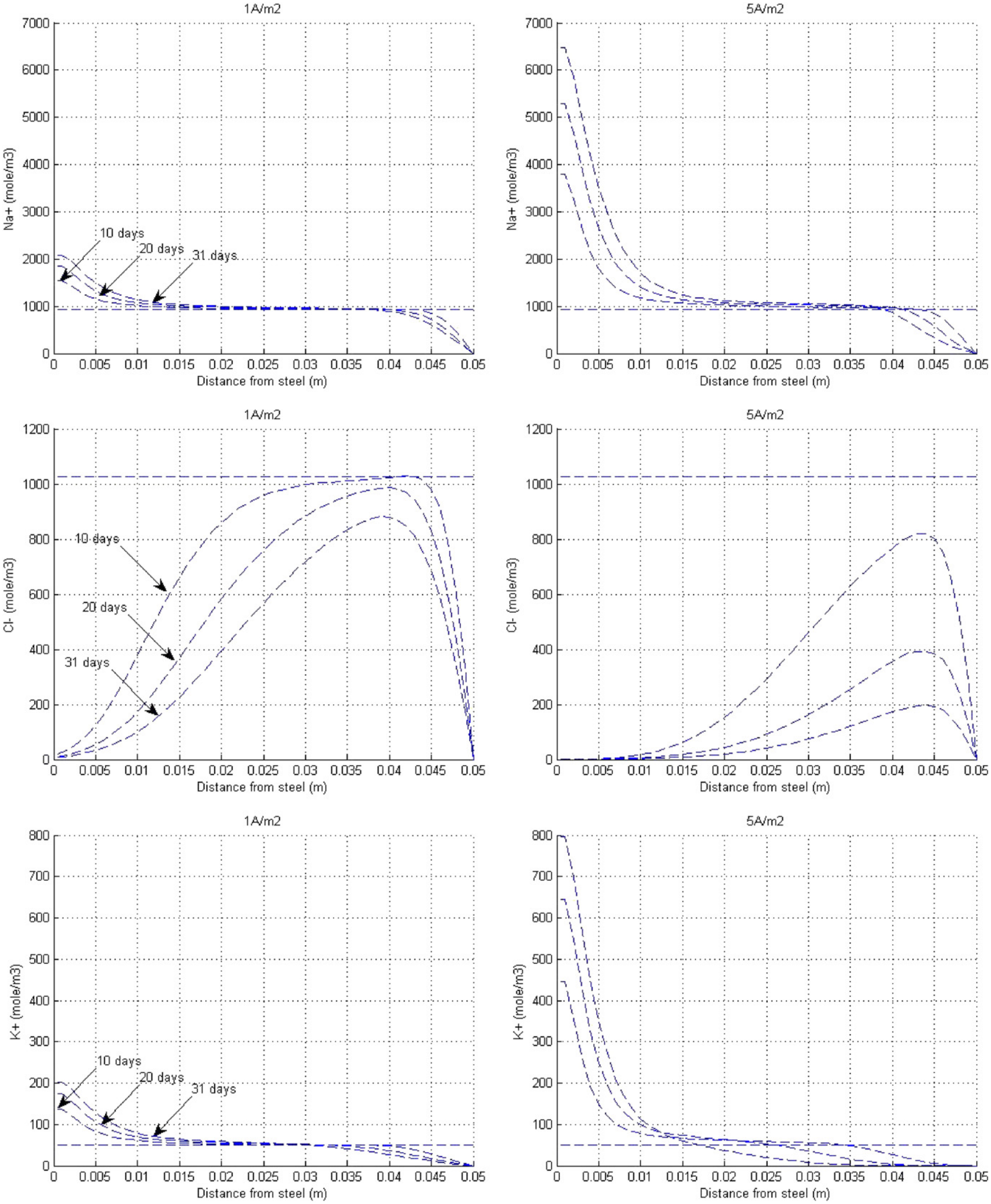

Fig. 8. Concentration profiles of various ionic species.

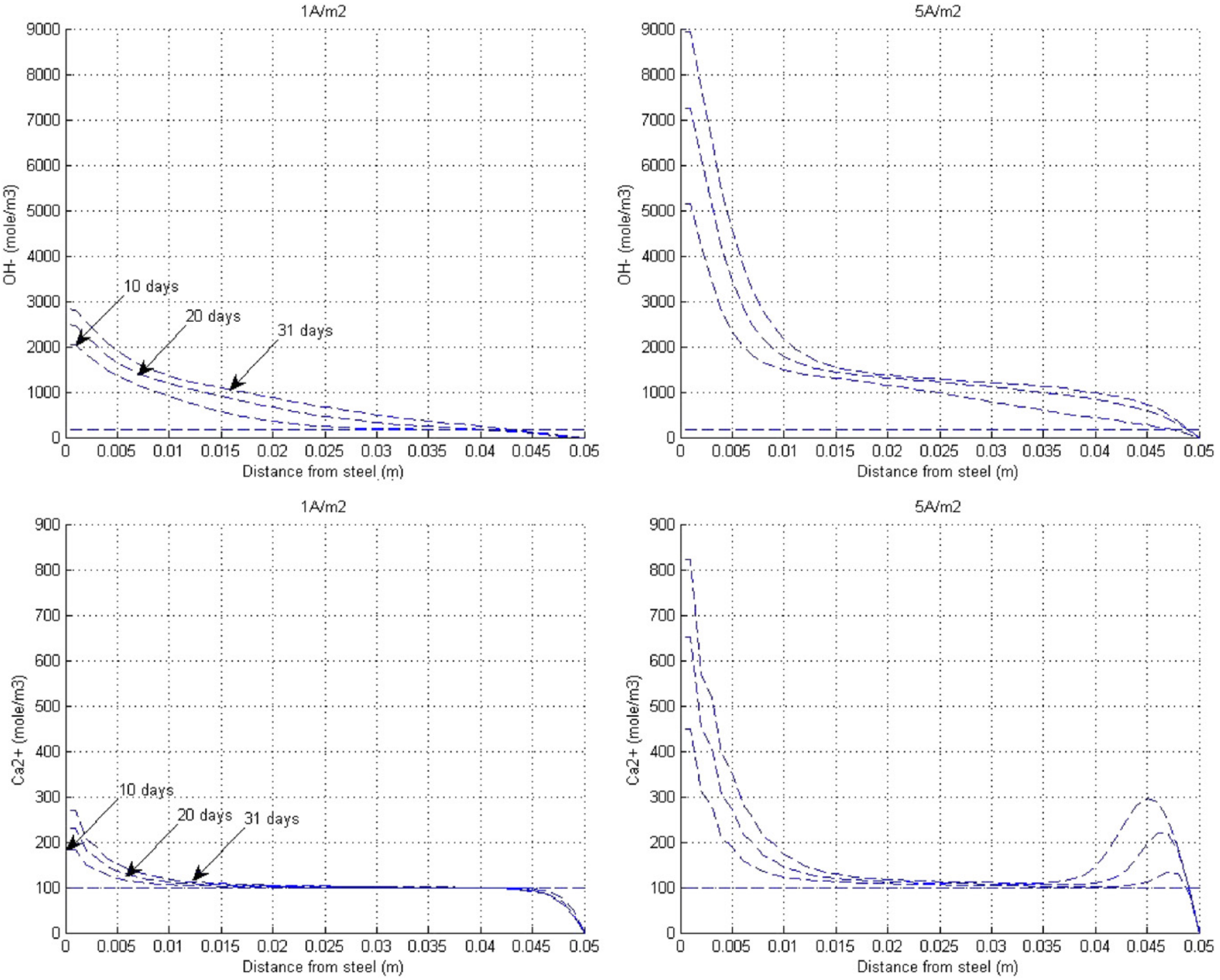

Fig. 8 (*continued*).

density leads to a rapid increase of the potassium and sodium ions in the region of the steel cathode;

3. The binding isotherm plays an important role in the prediction of chloride removal and the binding is a limiting factor of chloride removal.

## Acknowledgement

The authors would like to thank C. Andrade from 'Instituto Eduardo Torroja' of Madrid, for her collaboration in the determination of the concrete pore solution composition by the pore pressing technique.

## References

[1] A. Bautista, J.A. Gonzalez, Analysis of the protective efficiency of galvanizing against corrosion of reinforcements embedded in chloride contaminated concrete, Cement and Concrete Research 26 (2) (1996) 215–224.

[2] F. Belaid, G. Arliguie, R. François, Corrosion products of galvanised rebars embedded in chloride-contaminated concrete, The Journal of Science and Engineering Corrosion 56 (9) (2000) 960–965.

[3] F. Belaid, G. Arliguie, R. François, Effect of bars properties on bond strength of galvanised reinforcement, ASCE Journal of Materials in Civil Engineering 13 (6) (2001).

[4] A. Zayed, A. Sagues, R.G. Powers, Corrosion of epoxy-coated reinforcing steel, NACE Corrosion, vol. 189, 1989, (paper 379, Houston, Texas (USA)).

[5] B. Elsener, M. Buchler, F. Stalder, H. Bohni, Migrating corrosion inhibitor blend for reinforced concrete: Part1: prevention of corrosion, Corrosion 55 (1999) 1155–1163.

[6] B. Elsener, M. Molina, H. Bohni, The electrochemical removal of chlorides from reinforced concrete, Corrosion Science 35 (5–8) (1993) 1563–1570.

[7] J. Tritthart, Ion transport in cement paste during electrochemical chloride removal, Advances in Cement Research 11 (4) (1999) 149–160.

[8] T.D. Marcotte, C.M. Hansson, B.B. Hope, The effect of the electrochemical chloride extraction treatment on steel-reinforced mortar. Part I: electrochemical measurements, Cement and Concrete Research 29 (1999) 1555–1560.

[9] J.C. Orellan, G. Escadeillas, G. Arliguie, Electrochemical chloride extraction: efficiency and side effects, Cement and Concrete Research 34 (2004) 227–234.

[10] G. Fajardo, G. Escadeillas, G. Arliguie, Electrochemical chloride extraction (ECE) from steel-reinforced concrete specimens contaminated by "artificial" sea-water, Corrosion Science 48 (1) (2006) 110–125.

[11] O. Truc, J.P. Ollivier, Nilsson Lars-Olof, Numerical simulation of multi-species transport through saturated concrete during a migration test, Cement and Concrete Research 30 (2000) 1581–1592.

[12] E. Samson, J. Marchand, J.J. Beaudoin, Describing ion diffusion mechanisms in cement-based materials using the homogenization technique, Cement and Concrete Research 29 (8) (1999) 1341–1345.

[13] Q. Sa'id-Shawqi, C. Arya, P.R. Vassie, Numerical modeling of electrochemical chloride removal from concrete, Cement and Concrete Research 28 (3) (1998) 391–400.

[14] S. Chatterji, Transportation of ions through cement based materials. Part 1. Fundamental equations and basic measurement techniques, Cement and Concrete Research 24 (5) (1994) 907–912.

[15] L.Y. Li, C.L. Page, Modelling of electrochemical chloride extraction from concrete: influence of ionic activity coefficients, Computational Materials Science 9 (1998) 303–308.

[16] C. Andrade, J.M. Diez, A. Alaman, C. Alonso, Mathematical modelling of electrochemical chloride extraction from concrete, Cement and Concrete Research 25 (4) (1995) 727–740.

[17] L.Y. Li, C.L. Page, Finite element modelling of chloride removal from concrete by an electrochemical method, Corrosion Science 42 (2000) 2145–2165.

[18] L. Tang, Concentration dependence of diffusion and migration of chloride ions: Part 1: theoretical considerations, Cement and Concrete Research 29 (1999) 1463–1468.

[19] L. Tang, Concentrations dependance of diffusion and migration of chloride ions: Part 2: experimental evaluations, Cement and Concrete Research 29 (1999) 1469–1474.

[20] E. Samson, J. Marchand, Numerical solution of the Nernst–Planck model, Journal of Colloid and Interface Science 215 (1999) 1–8.

[21] R.S. Barneyback Jr., Sidney Diamond, Expression and analysis of pore fluids from hardened cement pastes and mortars, Cement and Concrete Research 11 (2) (1981) 279–285.

[22] O. Francy, Modélisation de la pénétration des ions chlorures dans les mortiers partiellement saturés en eau, PhD thesis, 1998.